An Adjoint Numerical / Empirical Approach to Predict the Total Resistance of Ships

Hulya Sukas[*1], Muhittin Kantaroglu[1], Omer Kemal Kinaci[1]

hulyaistif@gmail.com

[1] *Naval Architecture and Maritime Faculty, Yildiz Technical University, Istanbul, Turkey*

Abstract

This study aims to propose a fast calculation method to evaluate the total resistance of a traditional ship hull form. It became a common knowledge nowadays that the computational fluid dynamics (CFD) approach is robust in calculating the frictional resistance component of a ship with double body flow solutions. Modeling of the free surface is still a problematic issue due to the mathematical background of the Volume of Fluid (VOF) approach and even if a good match is obtained with experiments, these multiphase computations consume a lot of time and need higher computational power. To circumvent this problem, this study proposes a hybrid CFD-empirical approach. The results of the single phase computations obtained by CFD is coupled with the empirical approach of Holtrop-Mennen. The frictional and viscous pressure resistances of a benchmark ship (Duisburg Test Case – DTC) were calculated by CFD and using the wave resistance values of the Holtrop-Mennen resistance calculation method, the total resistance was obtained. To assess double body solutions dominated by viscosity, two different turbulence models were evaluated in the process. It was found out that k-omega turbulence model generated slightly better results compared to the k-epsilon according to the reference experiments.

Keywords: ship resistance, CFD, Hughes approach, Holtrop-Mennen

1. Introduction

Ship design is a sensitive and challenging field where almost all of the basic engineering principles are used. Theoretically small mistakes which can lead to inactivity in practice are quite extensive in the shipbuilding industry. Such problems can be understood when the ship is in operation, so it is very difficult to recover from mistakes. The paths followed in the preliminary design stage should be as follows:

- Determination of dimensions according to load capacity and speed value of the ship
- Strength calculations
- Determination of resistance and propulsion characteristics
- Stability and seakeeping characteristics

The initial design of a ship generally includes three stages:

- Concept Design

- Preliminary Design
- Contract Design

The process of initial design is often illustrated by the famous design spiral which indicates the objectives of the design. It is left to the designers' effort and experience to get the best solution adjusting and balancing the interrelated parameters.

A concept design should provide sufficient information for a basic techno-economic assessment. Economic criteria that may be derived for commercial ship designs and used to measure their profitability are net present value, discounted cash flow or required freight rate. Preliminary design refines and analyzes the agreed concept design.

Resistance and propulsion are crucial in ship design. One of the critical objectives of the preliminary design stage is to accurately calculate the resistance and propulsion characteristics of the conceptually designed ship. Vessels are built according to the specifications that are required by the customer. The design criteria are based on the contract signed between the shipyard and customer and the construction of the ship begins according to this agreement. In the case where contract conditions are not met by the shipyard, financial sanctions apply. Therefore, shipyards need quick estimation of the hydrodynamic characteristics of a planned ship during this stage to order the main engine. Fast and precise results lead to correct main engine orders that match the requirements of the technical specification. In order to design the propulsion system, the hydrodynamic characteristics of the vessel must be known. It is very difficult to determine these hydrodynamic characteristics because ships have complex geometries that are subjected to turbulence due to working at very high Reynolds numbers. Despite this turbulent flow regime which alters many numerical approaches, the resistance of the ship should be correctly calculated to assess the necessary main engine power accurately.

This study focuses on a fast and practical approach to calculate the total resistance of a ship prior to the selection of the main engine. A method is presented to calculate the total resistance of a ship that joins together empirical and numerical methods to speed up the calculation processes.

2. Ship resistance

A designer who deals with a new construction has several methods available for calculating the ship resistance.These methods, as shown in the figure 1, extend from traditional resistance methods to computational fluid dynamics(CFD) methods .

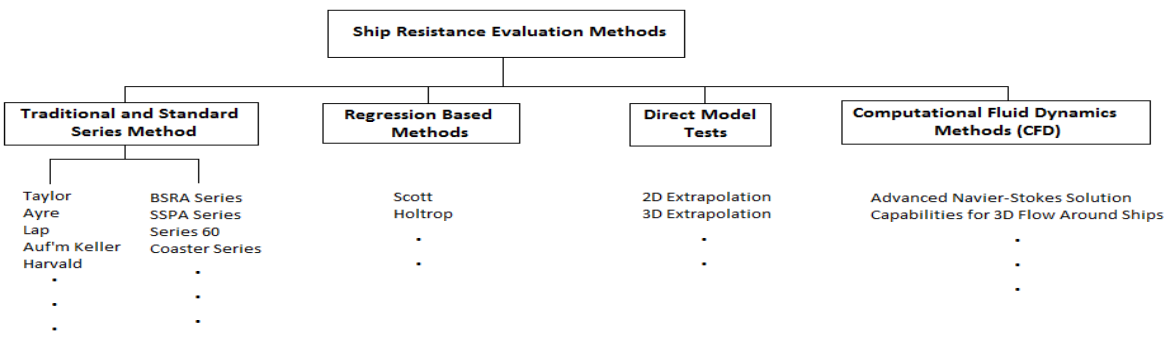

Figure 1. Ship resistance evaluation methods (Molland, 2008).

As it is shown in figure1, ship resistance evaluation methods can be categorized into four basic approaches. Except CFD and direct model test approaches, other methods are based on traditional parameters on ocean engineering such as block coefficient, longitudinal center of buoyancy, prismatic coefficient etc. Although these form parameters have been used for a period of conventional resistance calculations, as requirements have become more exact, these parameters less reflect the change in resistance components as vessel geometries become more complex. This is one of the reasons of CFD finding itself a solid ground in ship resistance calculations. The others may be stated as the expensive cost of experiments and easy access to faster computers by researchers working in this field.

The ship resistance consists of two components; pressure resistance and friction resistance. It would not be wrong to call this type of a categorization as an “artificial distinction” because resistance components are interrelated and impossible to totally break up. However, it provides a solid ground for various approaches to be made and ease calculations. Friction resistance is caused by viscosity-induced tangential forces acting on the ship's surface which is generally calculated either empirically or numerically. ITTC correlation line provides a useful equation that relates frictional resistance coefficient to the Reynolds number for ships. Pressure resistance is due to the vertical forces acting on the surface normal. Wave formation is inevitable due to ships working in a two-phase (water and air) environment. The waves formed by the ship itself and the waves coming onto the ship also contribute to resistance. These resistance components that are all related to free surface deformations are part of the pressure resistance. It is one of the problematic issues of naval architecture to totally discretize and calculate wave resistance component, whether numerical or experimental.

From a theoretical point of view, if a vessel is moving in a viscous flow (water + air) at a specified velocity, pressure and frictional forces act on the vessel. The total resistance is composed of the two different force components:

$$R_T = \int (T_x + N_x) dS \tag{1}$$

where R_T is the total resistance, S is the wetted surface area, T_x is the component in x direction of the tangential frictional force and N_x is the component in x direction of the normal pressure force acting on the ship. For the coordinate system, please see figure 2.

3. The method

This study proposes an adjoint method to calculate the total resistance of ships. Numerical and empirical results were partially used and superposed to obtain the total resistance. The viscous resistance R_V was calculated numerically and the wave resistance R_W was calculated empirically in the process. To start employing the method, the total resistance should be broken into its components first. There are different methods to approach the decomposition of total ship resistance problem. Towing tanks usually deploy Froude’s approach. In this study, Hughes’ approach was preferred for the numerical calculation of total ship resistance.

The numerical calculations were carried out for a double body flow condition that eliminates any perturbations on the free surface. With this approach, the wave resistance was completely eliminated from the numerical simulations and the total resistance obtained this way is equal to R_V.

The wave resistance component R_W was obtained by an empirical approach. The Holtrop-Mennen method calculates the total resistance of a ship by calculating the resistance components. Only the R_W value of the Holtrop-Mennen was used to estimate the total resistance. In this section, Hughes' method was briefly explained first and then the calculation procedure of the empirical approach was presented.

3.1. Hughes approach to ship resistance problem

G. Hughes, as a result of experimental study in the 1950s (Hughes, 1954), broke down the total resistance of a ship into three main components. These resistance components are; the wave resistance (R_W) due to gravitational forces, the frictional resistance (R_F) due to the viscosity of the fluid and the viscous pressure resistance (R_{VP}) due to the underwater hull form. Since these three resistance components cannot be measured separately, he combined the frictional and viscous pressure resistance which depend on the Reynolds number and called this force component as the viscous resistance (R_V). Hence in the Hughes approach, the total resistance of a ship (R_T) can be divided into its components as viscous resistance and wave resistance (Molland, 2008).

$$R_T(Rn, Fn) = R_F(Rn) + R_{VP}(Rn) + R_W(Fn) \quad (2a)$$

$$R_V(Rn) = R_F(Rn) + R_{VP}(Rn) \quad (2b)$$

$$R_T(Rn, Fn) = R_V(Rn) + R_W(Fn) \quad (2c)$$

As given in equation set (2), frictional resistance is only a function of the Reynolds number and its coefficient$C_F$is easy to calculate using ITTC correlation line formula (ITTC 7.5 – 02 – 03 – 01.4) which is given as:

$$C_F = \frac{0.075}{(\log Re - 2)^2} \quad (3)$$

and using this equation frictional resistance is calculated by the formula:

$$R_F = \frac{1}{2}\rho S V^2 C_F \quad (4)$$

Here V is the ship velocity and ρ is the density of water. The viscous pressure resistance is found by multiplying the calculated friction resistance with a constant coefficient k. This value, which is completely dependent on the form of the ship, is called as the form factor. Although recent research proved otherwise (Gomez, 2000), in this approach it is assumed that k is not changing with the Reynolds number or the model scale.

$$R_V = R_F + R_{VP} = (1 + k)R_F \quad (5)$$

The method of Prohaska is used in the towing tanks to obtain the form factor k of the ship. The ship is towed at several velocities that are very close to zero and the form factor at zero velocity is calculated using various numerical methods. However RANSE based CFD provides a shortcut to directly calculate the form factor of a ship. Calm free water surface which is *only theoretically possible* can be dictated to the solver by only modeling the underwater hull and assuming that there is only water in the medium; ignoring the air and the interface in between (this is called "single phase" analysis).

3.2. The empirical Holtrop-Mennen method

Holtrop-Mennen is a widely used empirical model to predict total resistance of ships. The method can predict a wide range of hull forms including its appendages and is generally based on Hughes approach to resistance problem. The total resistance in Holtrop-Mennen method is divided into:

$$R_T = R_F(1+k) + R_W + R_{APP} + R_B + R_{TR} + R_A \quad (6)$$

The first two terms on the right hand side are the same as in Hughes' approach. The third (R_{APP}), fourth (R_B), fifth (R_{TR}) and sixth (R_B) terms are resistance components that arise from appendages, bulbous bow, transom stern and model-ship correlation respectively. In this study we will only use the wave resistance term R_W of the empirical Holtrop-Mennen method. The details of calculation of R_W can be found in the reference article (Holtrop and Mennen, 1982).

4. Validation of the empirical method

The Holtrop-Mennen empirical method was first tested using the experimental and numerical results of Sukas et al. (2016). The comparison is given in figure 2.

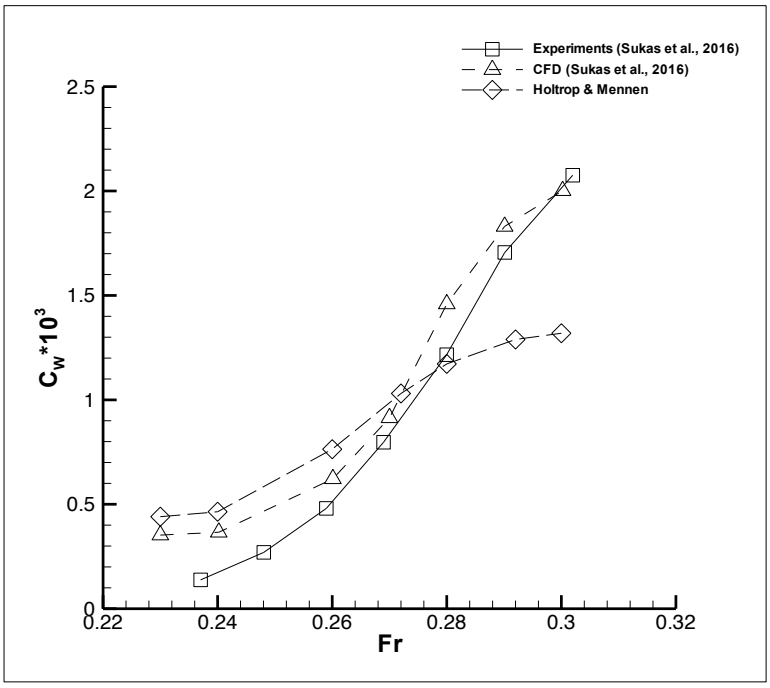

Figure 2. Comparison wave resistance coefficients of KCS for different Froude numbers.

The empirical method generates higher values for wave resistance coefficient at lower Froude numbers but lower values at higher Fr. The increase in C_W is monotonic empirically although experimental and numerical results suggest a sharper increase with respect to Fr. However, Holtrop-Mennen method is found to be very practical and it is believed that it gives a notion about the wave resistance.

5. Numerical setup

In this chapter, the hull used in the CFD simulations is described along with numerical simulation details. The Duisburg Test Case (DTC) model was the hull used for all of the numerical simulations reported in this study. The experimental data of the benchmark ship and some other numerical results were used to validate the CFD results. The geometric properties of the ship are given in table 1 and a perspective view of the underwater hull is shown in figure 3.

Figure 3. Perspective view of the underwater hull of the DTC model.

Firstly, the pre-processing of the simulation was done and the fluid domain which is shown figure 4 was modeled by using software Rhinoceros 3D. The dimensions of the computational domain were determined using the recommended procedures and guidelines of the ITTC for practical ship CFD application (ITTC 7.5 – 03 – 02 – 03).

Table 1. Main dimensions of the model size and full-scale ship.

λ= 59.407	**Model Size**	**Full-Scale**
L (m)	5.976	355
B (m)	0.859	51
T (m)	0.244	14.5
V (m^3)	0.827	173467
C_B	0.661	0.661
S_W (m^2)	6.243	22032

After making sure that the volume was enclosed, it was exported into the Star CCM+ to carry out the numerical simulations. The boundary conditions of the domain surfaces in figure 3 are given in table 2.

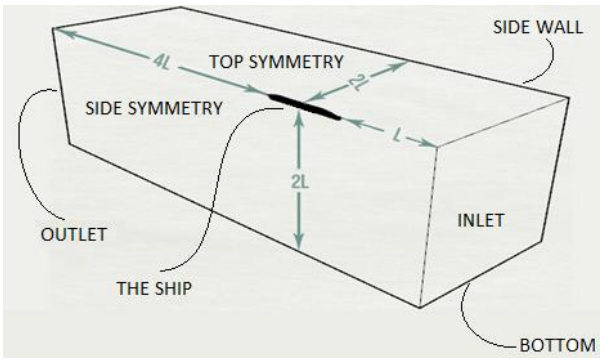

Figure 4. Computational domain extents with respect to ship length and the domain surfaces.

Dictating the symmetry condition means that the no-slip wall condition is not applied on the

boundary. This means that when the fluid passes over the surface, it flows without shear stresses. If we chose a wall condition instead of symmetry, for example for the bottom side, the velocity of the fluid would be equal to zero on that surface. Although the boundaries were chosen to be satisfactorily far away, symmetry condition was applied so that they would have no influence on the hull. That's why the symmetry condition was chosen for bottom and side wall. The vessel was split into two and only half of it was solved to decrease the number of elements in the fluid domain and this was done by giving the side symmetry, a symmetry boundary condition. The symmetry condition for the top side, on the other hand, was given so that the vessel would not get influenced by any free water surface deformations. The symmetry boundary condition for the top side imposed a double body flow condition for the solver. This implies that only the underwater part of the hull is modeled and solved.

Table 2. Boundary conditions imposed on the solver.

DOMAIN SURFACE NAME	BOUNDARY CONDITION
Inlet	Velocity Inlet
Outlet	Pressure Outlet
Top Symmetry	Symmetry
Bottom	Symmetry
Side Symmetry	Symmetry
Side Wall	Symmetry
Hull	Wall

Model selection to create an accurate grid system was done under the meshing module. In marine problems, surface re-mesher option was activated as the surface of the hull is complex. Additionally, trimmer mesh module was chosen. The general view of the grid system for the computational domain is indicated in figure 5. In that figure, the ship is at the upper right side of the picture where there is a thick mesh refinement.

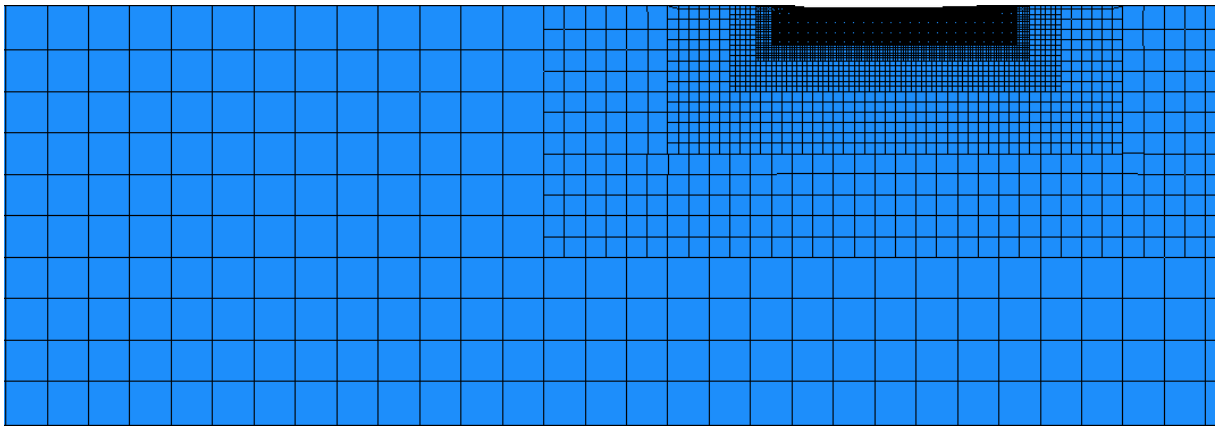

Figure 5. The rigid grid design for the computational domain (Side view).

The boundary layer helps solving the turbulent flow around the hull accurately, thus it was activated in the solver. Because of the highly curved hull surface around the bulb, the boundary marching angle was set to 75^{o} to ensure that the prism layers can be drawn smoothly around the vessel. The

minimum proximity of 0.001 was entered on the automatic surface repair tab. This means that you can mesh in close proximity to the mesh values which were entered through the setup of the simulation. The grid size on the hull surface needs to be as small as possible to reflect the complexity of the ship geometry. The grid system created on the hull is shown in figure 6.

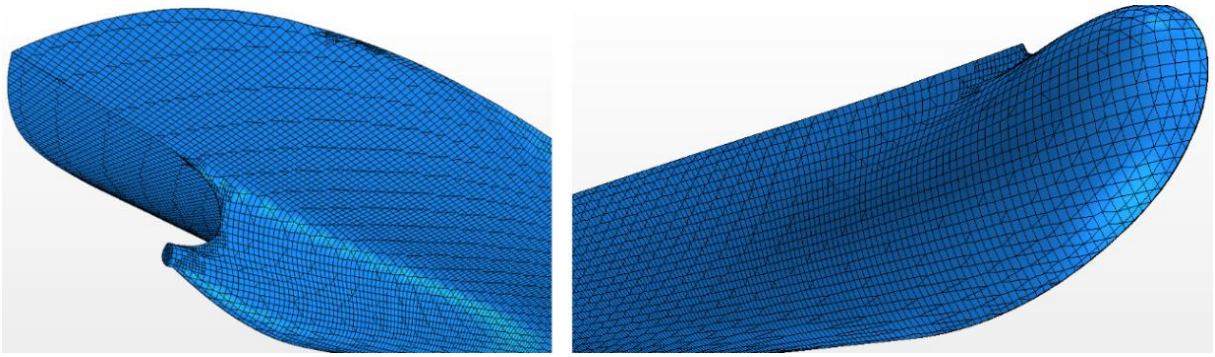

Figure 6. The grid system on the stern (left) and bow (right) of the ship.

The maximum element size was determined as 400% of the base size value. These elements will usually be located on the domain boundaries. Six prism layers were used to solve the flow in the boundary layer. The maximum boundary layer thickness was calculated by an empirical formula (Schlichting, 1968), which is given as;

$$\delta_{max} \approx \frac{0.37L}{\sqrt[5]{Re_{max}}} \tag{7}$$

Here, δ_{max} represents the maximum boundary layer thickness which is expected at the very aft of the ship (which is a distance of L from the point where the flow meets the ship). At this particular point $Re = Re_{max}$. The value obtained from equation (7) for the maximum boundary layer thickness is given as an input to the code. The prism layer on the hull is shown in figure 7. Template growth rate and boundary grow rate were changed to “slow”. Enabling this option means that mesh elements in the control volume grow slowly in size through the far areas.

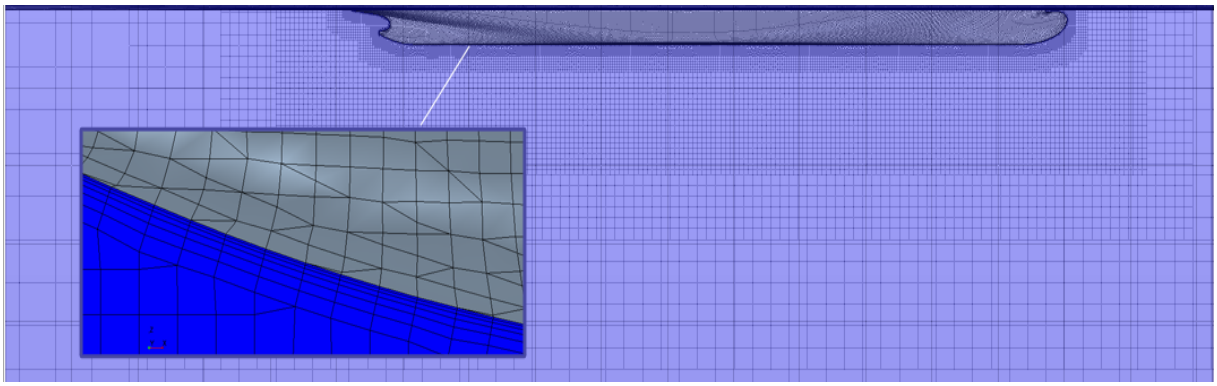

Figure 7. A zoomed-in view of the prism layer around the hull.

Volumetric controls for refining the grid at certain places of the hull were created by adding blocks to critical zones. These zones usually cover the highly curved places of the hull due to chaotic flow

expectation (cross flows, reversed flows, high pressure gradients etc. see figure 8). Surface re-mesher and isotropic trimmer option was chosen for the hull vicinity. Isotropic trimmer means; the elements are equally re-meshed along x, y, z directions.

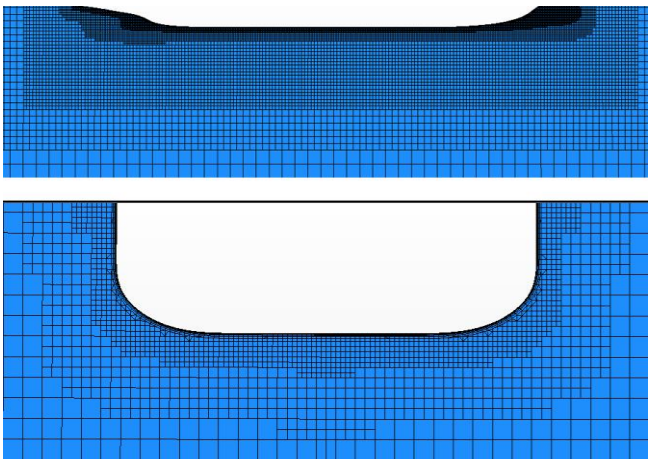

Figure 8. Volumetric controls created to acquire an accurate prediction of the flow around the hull.

The maximum element sizes were set to be at the boundaries and were in relation with the base grid size value. For this study, the total number of mesh elements is about 750K.

Table 2. Physical model used for the double-body case in Star-CCM+.

Flow property:	Steady State
Material used:	Water (Constant Density)
Flow model:	Segregated Flow
Viscous regime:	Turbulent
Turbulence model:	$k-\varepsilon$ & $k-\omega$
Number of prism layer:	6
Gradient method:	Hybrid Gauss-LSQ

The physical model which can be shown in table 2 was set up after the meshing process was totally completed. In our problem, the flow around the hull was solved independent of time. Since the free surface effects were not included in this work, it is found to be reasonable to choose a steady solution to achieve faster results. Due to the nature of single-phase analyses, only water was selected as fluid and gravitational acceleration was not activated. For the property of the fluid flow, segregated flow option was enabled. Fluid density was chosen as being constant. Viscous regime was chosen as turbulent. $k-\varepsilon$ and $k-\omega$ turbulence models were selected and the results obtained from the two turbulence models were compared in the study.

6. Results

As it was mentioned before, in this study two different turbulence models were used to obtain the total resistance of the hull. Initially, $k-\varepsilon$ turbulence model was used and the results of this model

are given in table 3. These results were obtained by only simulating the double-body simulations as explained in previous sections. The wave resistance values calculated by the Holtrop-Mennen method were added to the double-body CFD results and then the total resistance values were obtained as shown in table 4.

Table 3. The results obtained by double-body CFD using the $k-\varepsilon$ turbulence model.

Fr	$(R_T - R_W)$	R_F	R_{VP}	$(C_T - C_W)x10^3$	$C_F x10^3$
0.174	17.727	16.378	1.349	3.096	2.861
0.183	19.329	17.862	1.467	3.066	2.833
0.192	21.051	19.457	1.594	3.037	2.807
0.200	22.791	21.068	1.723	3.011	2.784
0.209	24.626	22.770	1.856	2.987	2.762
0.218	26.504	24.510	1.994	2.966	2.743

Table 4. The total resistance results including the wave resistance component by the Holtrop-Mennen method on top of table 3.

Fr	R_W	R_P	R_T	$C_T x10^3$
0.174	0.642	1.991	18.369	3.221
0.183	1.007	2.474	20.336	3.238
0.192	1.420	3.014	22.471	3.255
0.2	1.826	3.549	24.617	3.265
0.209	2.607	4.463	27.233	3.317
0.218	3.801	5.795	30.305	3.404

$k-\omega$ turbulence model was adopted in the numerical simulations as a second step and the results are given in table 5. The wave resistance values calculated by the Holtrop-Mennen method were added to the double-body CFD results and then the total resistance values were acquired. Total resistances in this case are given in table 6.

Changes in C_F depending on the Froude number can be examined in figure 9. The figure shows that the results of the numerical simulations performed with the $k-\omega$ turbulence model were slightly closer to the empirical ITTC correlation line formula which was given in equation (3).

According to the results obtained in these cases, changes in C_T with respect to the Froude number is shown in figure 10. Although there was a discrepancy between the ITTC correlation line and the numerical simulations in terms of the frictional resistance coefficient results, it was partially compensated by the difference between the Holtrop-Mennen empirical method and the experimental results.

Table 5. The results obtained by double-body CFD using the $k-\omega$ turbulence model.

Fr	R_T - R_W	R_F	R_{VP}	$(C_T - C_W)x10^3$	$C_F x10^3$
0.174	20.944	19.501	1.442	3.658	3.406
0.183	22.737	21.173	1.564	3.606	3.358
0.192	24.651	22.958	1.693	3.556	3.312
0.200	26.573	24.749	1.824	3.511	3.270
0.209	28.588	26.628	1.960	3.468	3.230
0.218	30.637	28.539	2.098	3.428	3.193

Table 6. The total resistance results including the wave resistance component by the Holtrop-Mennen method on top of table 5.

Fr	R_W	R_P	R_T	$C_T x10^3$
0.174	0.642	2.084	21.585	3.785
0.183	1.007	2.571	23.744	3.781
0.192	1.420	3.113	26.071	3.776
0.2	1.826	3.650	28.399	3.767
0.209	2.607	4.567	31.195	3.799
0.218	3.801	5.899	34.438	3.869

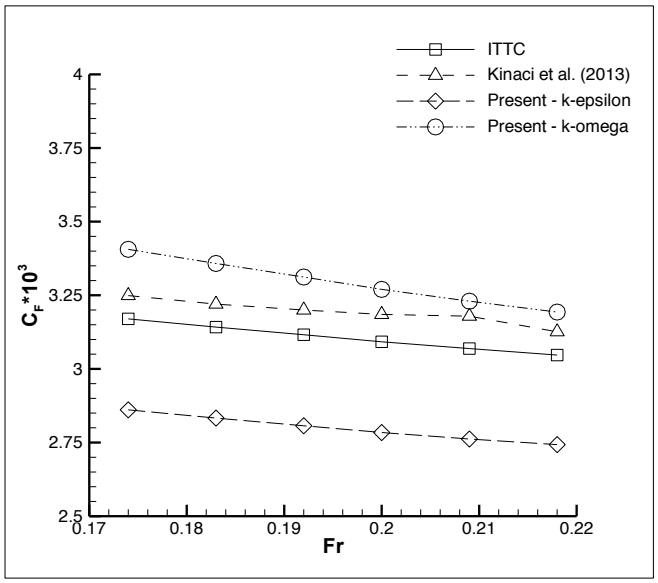

Figure 9. Fr versus C_F using two different turbulence models.

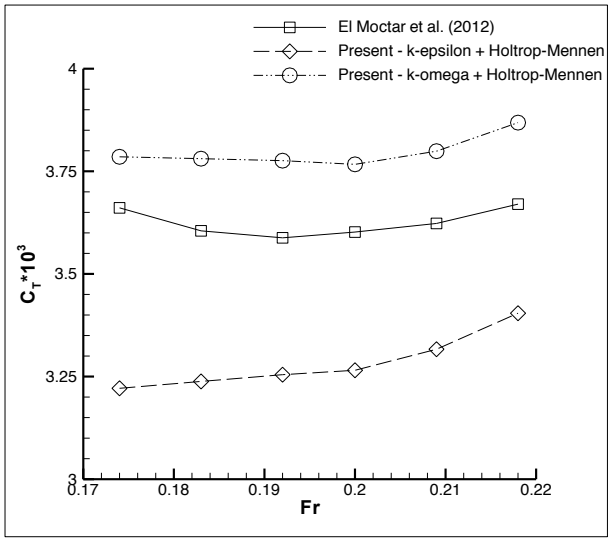

Figure 10. Fr versus C_T using two different turbulence models and the Holtrop-Mennen method.

The C_W results calculated with the empirical formula in this study (Holtrop-Mennen) and the experimental data are compared in figure 11. Experimental results suggested a hump in wave resistance coefficient whereas the empirical Holtrop-Mennen method suggested a logarithmic increase. The empirical results were lower compared to the experiment in lower Froude numbers while it wads vice versa at the service speed of the vessel ($Fr = 0.218$).

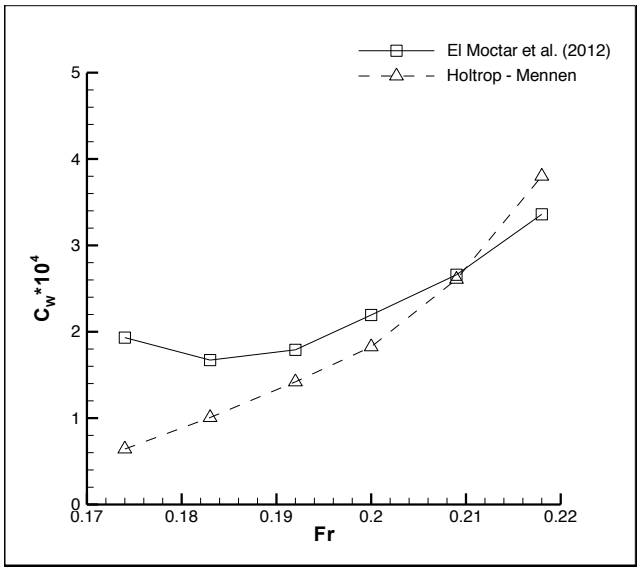

Figure 11. Comparison of C_W between the empirical and experimental results.

7. Conclusion

This study aims to propose an adjoint empirical/numerical approach to assess the total resistance of ships. The method was based on Hughes' approach to resistance problem where the total resistance is divided into its components including the wave resistance. The wave resistance was estimated using an empirical Holtrop-Mennen method while the other components (frictional resistance and

the viscous pressure resistance) were calculated via a fully nonlinear numerical method that can take turbulence into account.

Wave resistance was neglected in numerical simulations by assuming that there were no deformations on the free surface. A single phase numerical simulation that only takes into notice the underwater hull form of the ship returns the sum of frictional resistance and the viscous pressure resistance. The outputs of the numerical results were then added to the wave resistance value generated by the Holtrop-Mennen method. This proposed hybrid approach is a practical way to approach the problem of determining the total resistance of a conventional ship. The classical method of CFD approach by making a multi-phase analysis including the free surface effects consumes a lot of time and computer memory. Moreover, it is hard to get converged results at low Froude numbers.

The classical experimental method neglects the dependency of form factor on Reynolds number; however, in this methodology, the form factor of the hull was not calculated. Single phase analysis automatically resolves the issue of ‘‘zero wave resistance inclusion’’ inside the total resistance during the form factor calculation. In a single phase analysis, the ratio of viscous pressure resistance to frictional resistance directly gives the form factor (1 + k) value of the ship which is dependent on the Reynolds number.

References

El Moctar, O., Shigunov, V., Zorn, T., (2012). Duisburg Test Case: Post-Panamax container ship for benchmarking. Ship Technology Research, 59, pp. 50-64.

Garcia-Gomez, A., (2000). On the form factor scale effect. Ocean Engineering, 27(1), pp. 97-109.

Holtrop, J. Mennen, G. G., (1982). An approximate power prediction method. International Shipbuilding Progress, 29, pp. 166-170.

Hughes, G. (1954). Friction and form resistance in turbulent flow and a proposed formulation for use in model and ship correlation. Transactions of RINA, 96.

International Towing Tank Conference (ITTC), (2011b). 7.5-03-02-03. Practical guidelines for ship CFD applications. In: Proceedings of the 26th ITTC.

Kinaci, O. K., Kukner, A., Bal, S., (2013). On propeller performance of DTC Post Panamax Container Ship. International Journal of Ocean System Engineering, 3(2), pp. 77-89.

Molland, A. (ed.), (2008). The maritime engineering reference book – a guide to ship design, construction and operation. Elsevier Ltd.

Schlichting, H., (1968). Boundary layer theory, Mc-Graw Hill, New York.

Sukas, O.F., Kinaci, O.K., Bal, S., (2016). Prediction of wave resistance by a Reynolds-averaged Navier Stokes equation-based computational fluid dynamics approach. Proceedings of the Institution of Mechanical Engineers – Part M: Journal of Engineering for the Maritime Environment, 230(3), pp. 531-548.

* Corresponding author.